Proceedings of Ninth World Conference on Earthquake Engineering
August 2-9, 1988, Tokyo-Kyoto, JAPAN (Vol.II)

3-7-6

PREDICTION OF EARTHQUAKE ACCELEROGRAMS OF STIFF GROUND BASED ON NONSTATIONARY AR-MA PROCESS

Joji EJIRI and Yozo GOTO

Technical Research Institute, Ohbayashi Corporation, Tokyo, Japan

SUMMARY

This paper presents the results of study for a prediction model for synthesizing earthquake accelerograms of stiff ground in Japan having nonstationary characteristics.

At first, it was assumed that earthquake accelerograms could be expressed by the nonstationary second order auto-regressive moving average (AR-MA) process and then the nonstationary characteristics of earthquake accelerograms were extracted as AR-MA parameters from 88 accelerogram records. Then, those nonstationary parameters were expressed by simple time functions to obtain the parameters constituting their time functions. Finally, the attenuation laws of these time function's parameters with relation to magunitude M and epicentral distance Δ were derived from a regression analysis.

The applicability of the attenuation laws was examined using mean response spectra obtained from predicted accelerograms.

INTRODUCTION

When performing a linear or nonlinear earthquake response analysis of a structure including adjacent ground, it is required to estimate characteristics of input earthquake motion appropriately such as not only maximum intensity but also nonstationary intensity, frequency and duration time of itself. In the common earthquake response analysis, the suitably modified waves have been practically used as an input earthquake motions based on the maximum intensity and frequency characteristics of the representative records such as EL Centro 1940 NS, Taft 1952 EW and so on. However, these records are likely to be affected by the dynamic properties of ground at the observed site and the parameters, M and Δ corresponding to the records may be uniquely involved.

In the present study, the prediction model was proposed to synthesize earthquake accelerograms with nonstationary characteristics in which both M and Δ and the specific ground condition were taken into account.

PREDICTION MODEL

Modeling of Nonstationary Earthquake Accelerograms An earthquake accelerogram can be modeled with a stochastic time series based on the nonstationary second order auto-regressive moving average (AR-MA) process as follows ;

$$Y_t = -\alpha_1(t)\cdot Y_{t-1} - \alpha_2(t)\cdot Y_{t-2} + \varepsilon_t + \beta_1(t)\cdot\varepsilon_{t-1} + \beta_2(t)\cdot\varepsilon_{t-2} \quad (1)$$

in which ε_t is the input white noise, Y_t is the observed earthquake accelerogram, $\alpha_i(t)$, $\beta_i(t)$ $(i=1,2)$ are nonstationary AR-MA parameters. This means that a synthesized accelerogram is an output of a single degree of freedom system excited by a nonstationary white noise as shown in Fig. 1.

The parameters $\alpha_i(t)$ are related to the natural frequency f(t) and the damping foctor h(t) of a single degree of freedom system as follows (Refs.1,2) ;

$$\lambda^2+\alpha_1\lambda+\alpha_2=0, \quad \left.\begin{matrix}\lambda \\ \lambda^*\end{matrix}\right\} = \exp\left(-2\pi f\, hTs \pm i2\pi f\, Ts\sqrt{1-h^2}\right) \quad (2)$$

in which $i = \sqrt{-1}$, λ and λ^* are cojugate complex solutions of the quadratic equation and Ts is the sampling interval with value of 0.02 second.

It is not easy to estimate the nonstationary AR-MA parameters $\alpha_i(t)$, $\beta_i(t)$ reasonably and so the rectangular window is multiplied to a given acceleration date series and the center point time τ_m of the window is assumed to be the time at which the AR-MA parameters are specified as shown in Fig. 2. 1 second was adopted for the window length Tw.

The filtering characteristics such as f(t) and h(t) of a single degree of freedom system can be calculated from the AR-MA parameters $\alpha_i(t)$, $\beta_i(t)$ which are determined by the two stage least square method proposed by Gersh (Ref.3). In the first least-square stage, the auto-regressive (AR) parameters are estimated by using the concept of maximum entropy method proposed by Burg (Ref.4).

Earthquake Accelerogram Records Analyzed and Their Correction on Instrumental Error A total of 88 sets of horizontal accelerogram records of 34 earthquakes were used in this analysis. They were observed between 1964 and 1980 for a period of 17 years at 17 free field sites on stiff ground (Group 1) (Ref.5) in Japan.

Fig. 3 shows the distribution of magunitude M and epicentral distance Δ. It is apparant that near-field records induced by large magunitude are quite few and that some records have small M-short Δ and the others have large M-long Δ.

Most of records analyzed were obtained with SMAC-B2 model accelerometers. The sensitivity at high frequency of this accelerometer is substantiarily low. Then correction on the instrumental error was performed using accelerometer's property and band-pass filter as shown in Fig. 4. Fig. 5 shows the relation between corrected and uncorrected peak accelerations. Corrected peak accelerations is 1.5 times on average as high as uncorrected ones.

Time Functions and Regression Analysis Fig. 6 shows an example of nonstationary characteristics of an observed accelerogram($M=6.7$, $\Delta=49$km) in which simulated accelerogram was synthesized using extracted AR-MA parameters directly and $\sigma(t)$ is input white noise intensity and it is likely to the envelope function of accelerogram. With the elapse of time f(t) seems to decrease and h(t) to increase respectively. In this way, after examining typical of accelerogram records, the nonstationarity of the AR-MA parameters were specified by simple time functions. The nonstationarities of parameters are given in Table 1. In this Table, σ_{max} and t_p are the maximum value of intensity and its occurence time respectively, and T is duration which is determined with the same

criteria (Ref.6).

The regression equations are provided by, with regard to σ_{max}, f_A and h_A

$$\log P = B_1 + B_2 \cdot M + B_3 \cdot \log(\Delta + 20) \quad (3)$$

and with regard to tp, f_B, h_B, $\overline{\beta_1}$, $\overline{\beta_2}$ and T

$$P = B1 + B2 \cdot M + B3 \cdot \log(\Delta + 20) \quad (4)$$

in which P stands for the parameters.

The regression analysis was made for each parameters in Table 1 using M and Δ.
The results of regression analysis is shown in Table 2, in which B1, B2 and B3 are regression coefficents and σp is standard deviation of the parameters for the regression equations. Fig. 7 shows the effect of M and Δ on some parameters.

RESULTS

Predicted accelerograms for M=6.5 at various Δ from constructed prediction model are shown in Fig. 8. When Δ becomes longer, peak accelerations decrease and T becomes longer.

Fig. 9 shows comparisons of absolute acceleration response spectra of earthquake accelerograms generated by applying various kinds of M and Δ to the constructed prediction model. When Δ becomes shorter, responses increase uniformly all over the period range. The predominant period in response spectra have no change in a range from 0.10 to 0.15 second. When M becomes larger, responses increase and predominant period tends to shift toward the long period range slightly. It is apparent that this tendency is more obvious in the long period range more than 0.15 second.

Fig. 10 shows a comparison with past attenuation models on stiff ground. The attenuation of the prediction model is not sensitive with Δ and has higher peak accelerations than others with the same M and Δ.

Fig. 11 shows a comparison with a typical design spectra for nuclear electric power plants in Japan. In the long period range more than 0.5 second, predicted spectra becomes larger than the design spectra. But in short period range, both spectra show a comparatively good agreement.

CONCLUSIONS

(1) The attenuations and spectral characteristics of predicted earthquake accelerograms coincided with the general trend of the earthquake motions recognized in past studies.

(2) It was ascertained that the natural frequency f(t) of earthquake motions of stiff ground decreased and the parameter h(t) of frequency distribution width increased with elapse of time. Such nonstationary characteristics were prominant for earthquakes with large M and small Δ.

(3) When the correction on instrumental error of the seismograph was added to the accelerograms of stiff ground, the peak acceleration increased 1.5 times on average and the response amplitudes of acceleration response spectra also increased. Moreover, the peak amplitude shifted to the short period side. This kind of correction should be made when analyzing earthquake accelerograms record obtained with SMAC-B2 model accelerometers commonly used in Japan.

ACKNOWLEDGMENTS

We would like to express our deep appreciation to Professor K. Toki and Associate Professor T. Sato of Disaster Prevention Research Institute of Kyoto University for the development of analysis used in this study. The accelerogram data given from the Public Works Research Institute, Ministry of Construction and the Port and Harbor Research Institute, Ministry of Transport are acknowledged.

REFERENCES

1. Toki, K., Sato, T. and Oiki, Y., Detection of Dynamic Properties of Structural Systems by the Autoregressive Moving Average Method, Annuals of Disaster Prevention Research Institute, Kyoto Univ., No.21 B-2, 57-68, 1978. (in Japanese)
2. Toki, K., Sato, T. and Ejiri, J., Simulation of Strong Motion Seismograms by Autoregressive Moving Average Process, Annuals of Disaster Prevention Research Institute, Kyoto Univ., No.23 B-2, 1-12, 1980. (in Japanese)
3. Gersh, W. and Livj, R.S.Z., Time Series Method for the Synthesis of Randam Vibrations Systems, Jour. Appl. Mecha, 159-165, 1976.
4. Burg, J.P., The Relationship between Maximum Entropy Spectra and Maximum Likelihood Spectra, Geophysics, 37, 375-376, 1972.
5. Japan Road Association, Design Code for Bridges, Earthquake Resistant Design, Vol. V, 1980. (in Japanese)
6. Trifunac, M.D. and Brady, A.G., A Study on the Duration of Strong Earthquake Ground Motion, BSSA, Vol.65, No.3, 581-626, 1975.

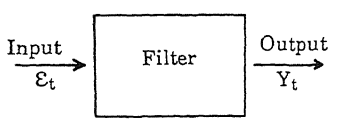

Fig.1 Filtering System

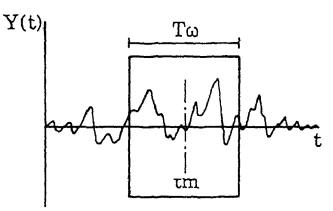

Fig.2 Expression for Nonstationarity

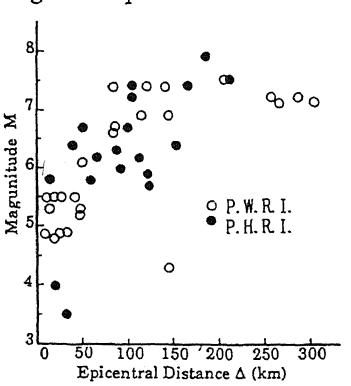

Fig.3 Distribution of M and Δ

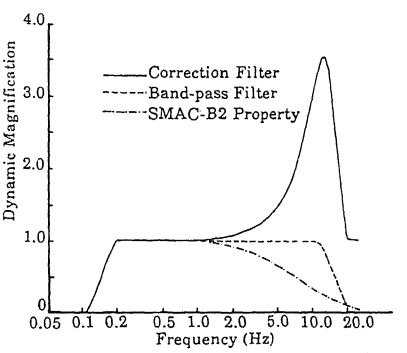

Fig.4 Frequency Characteristics of Correction Filter

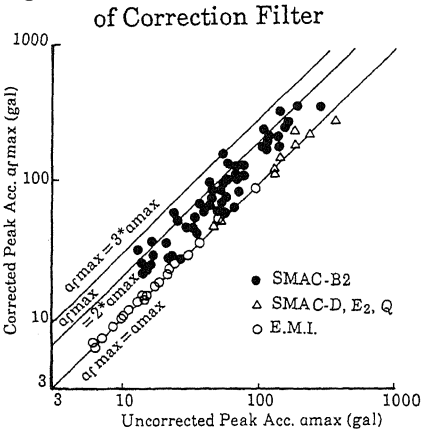

Fig.5 Relation Between Corrected and Uncorrected Peak Acc.

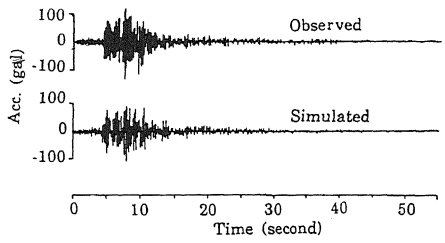

Observed and Simulated Accelerogram

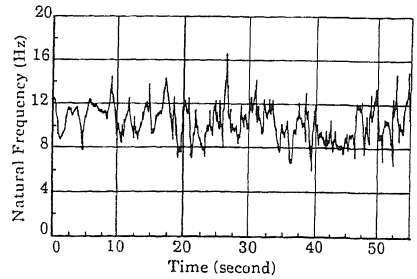

Natural Frequency f(t)

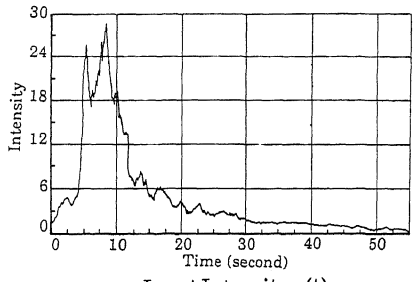

Input Intensity σ(t)

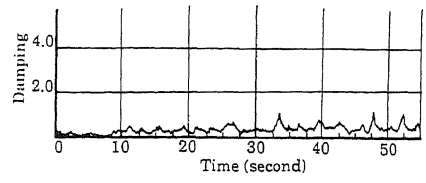

Damping h(t)

Fig.6 An Example of Nonstationary Characteristics

Table 1 Time Functions

$$\sigma(t) = \sigma_{max}(t/tp)\cdot\exp(1-t/tp)$$

$$f(t) = f_A\cdot\exp(-f_B\cdot t)$$

$$h(t) = h_A\cdot\exp(h_B\cdot t)$$

$$\beta_1(t) = \overline{\beta}_1 = \frac{1}{T}\int_0^T \beta_1(t)\,dt \quad \text{(const.)}$$

$$\beta_2(t) = \overline{\beta}_2 = \frac{1}{T}\int_0^T \beta_1(t)\,dt \quad \text{(const.)}$$

Table 2 Results of Regression Analysis

COEF. / P	B1	B2	B3	σ_p
log σmax	2.30	0.23	- 1.29	0.33
tp	- 26.55	2.46	8.70	6.82
log f_A	1.10	0.04	- 0.25	0.13
f_B	0.03	0.02	- 0.08	0.07
log h_A	- 1.00	0.04	0.03	0.29
h_B	-0.33	0.02	- 0.21	0.12
$\overline{\beta}_1$	0.37	0.001	- 0.007	0.26
$\overline{\beta}_2$	0.07	0.02	- 0.12	0.07
T	- 49.51	4.07	22.06	10.41

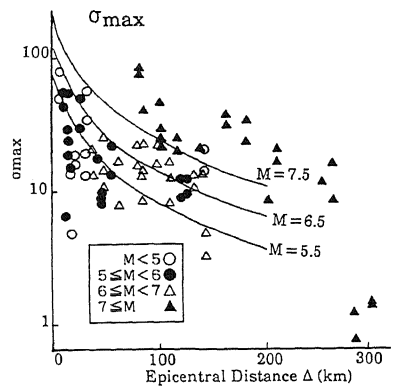

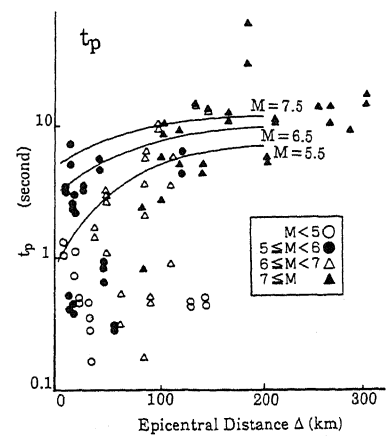

Fig.7 Effect of M and Δ

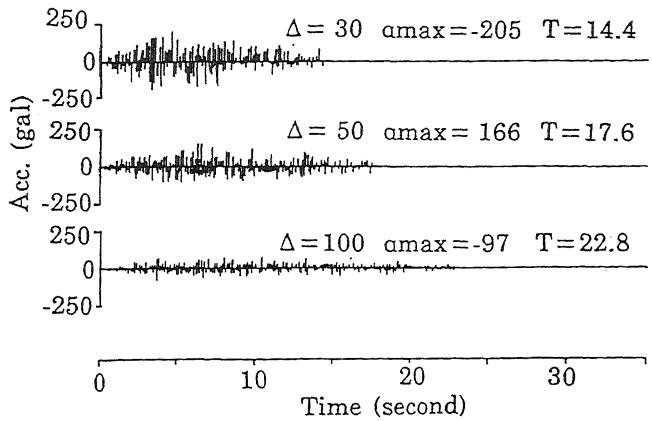

Fig.8 Predicted Accelerograms for M=6.5 at Various Δ

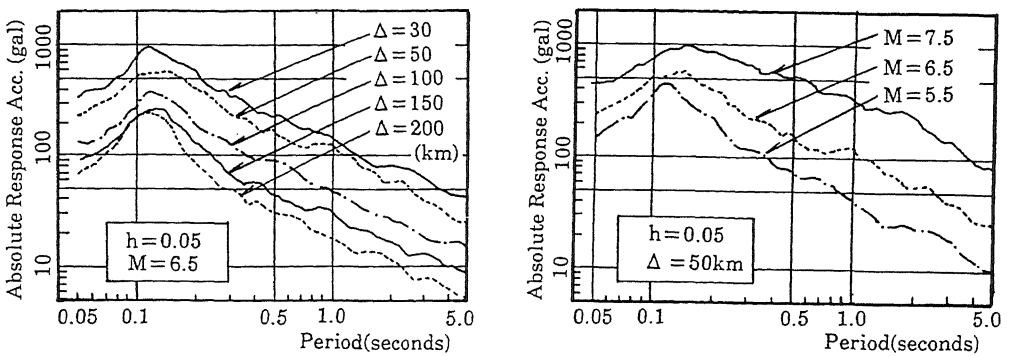

Predicted Acc. Spectra for M=6.5 at Various Δ

Predicted Acc. Spectra for Different M at Δ =50km

Fig.9 Comparison of Response Spectra

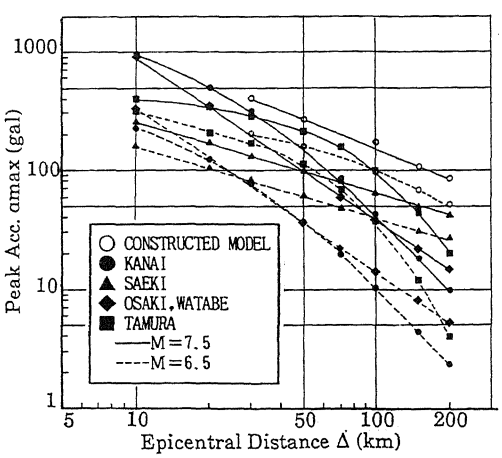

Fig.10 Comparison with Past Attenuation Models on Stiff Groun

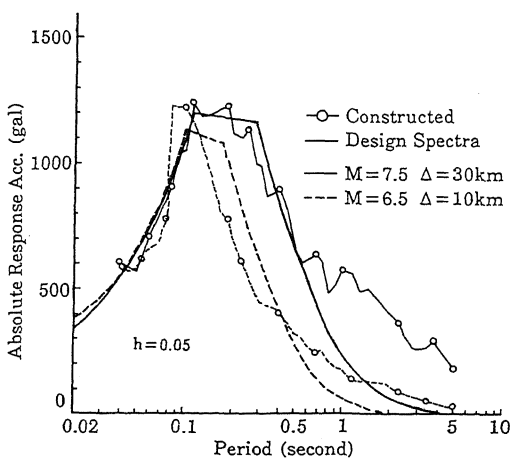

Fig.11 Comparison with Design Spectra